



HAL
open science

Impact of gold ion irradiation on the initial alteration rate of the International Simple Glass

C. Gillet, S. Szenknect, M. Tribet, H. Arena, S. Peugot

► **To cite this version:**

C. Gillet, S. Szenknect, M. Tribet, H. Arena, S. Peugot. Impact of gold ion irradiation on the initial alteration rate of the International Simple Glass. *Journal of Nuclear Materials*, 2024, 588, pp.154817. 10.1016/j.jnucmat.2023.154817 . hal-04679088

HAL Id: hal-04679088

<https://hal.science/hal-04679088v1>

Submitted on 27 Aug 2024

HAL is a multi-disciplinary open access archive for the deposit and dissemination of scientific research documents, whether they are published or not. The documents may come from teaching and research institutions in France or abroad, or from public or private research centers.

L'archive ouverte pluridisciplinaire **HAL**, est destinée au dépôt et à la diffusion de documents scientifiques de niveau recherche, publiés ou non, émanant des établissements d'enseignement et de recherche français ou étrangers, des laboratoires publics ou privés.

Impact of gold ion irradiation on the initial alteration rate of the International Simple Glass

C. Gillet^{a*}, S. Szenknect^b, M. Tribet^a, H. Arena^a and S. Peuket^{a*}

^a: CEA, DES, ISEC, DE2D, Univ Montpellier, Marcoule, France

^b: ICSM, Univ Montpellier, CEA, CNRS, ENSCM, site de Marcoule, Bagnols sur Cèze, France

*corresponding authors: celia.gillet@cea.fr (C. Gillet)

sylvain.peuget@cea.fr (S. Peuket)

Highlights

- ISG glass was irradiated with 7 MeV gold ions.
- Leaching experiments were performed on irradiated and non-irradiated samples.
- Initial alteration rate of ISG glass increased by a factor of 2 after irradiation with Au-ion.

Abstract

This study addresses the impact of 7 MeV Au irradiation on the initial alteration rate of International Simple Glass (ISG), considered as a reference for nuclear glasses. This irradiation scenario simulates the effect of nuclear collisions of the recoil nuclei of α decays. In order to study the very first moments of glass alteration, non-irradiated and Au-ion irradiated ISG glass monoliths were altered in pure water at 90°C, pH 9 and with a ratio of glass surface area to solution volume of 0.01 cm⁻¹. Glass alteration was monitored by measuring the releases of the glass elements in solution by UV-visible spectrophotometry and Inductively Coupled Plasma-Atomic Emission Spectroscopy (ICP-AES). Under these alteration conditions, the releases of the elements in solution are congruent. The initial

27 alteration rate was found to be (2.0 ± 0.8) times higher for the irradiated glass monoliths than for non-
28 irradiated samples.

29 Introduction

30 France has chosen to reprocess spent fuel in order to save part of the uranium resources through the
31 manufacture of MOx fuel. This recycling strategy also reduces the radiotoxicity of final waste as well
32 as its volume [1, 2]. In order to find a management solution suitable to each type of nuclear waste,
33 they are classified according to their level of radioactivity and lifetime [3]. High-level waste (HLW) are
34 packaged into a vitrified form and are intended for long-term disposal in a deep geological repository
35 (Cigeo project)[4, 5]. Once the waste packages are introduced into the disposal site, the glass will
36 initially evolve into a closed (free of water) system and will be subjected to its own self-irradiation due
37 to the fission products and minor actinides incorporated in the glass structure [1]. Fission products
38 produce β decays accompanied by γ transitions that predominate with respect to the total radioactivity
39 of the waste in the short term (after 100 years, beta/gamma and alpha activities are respectively of
40 around $7 \times 10^9 \text{Bq/g}$ and 10^8Bq/g), while α decays coming from actinide decays are the main contributor
41 to the activity for the long-term (after 1000 years, beta/gamma and alpha activities are respectively of
42 around $3 \times 10^6 \text{Bq/g}$ and $4 \times 10^7 \text{Bq/g}$) [6]. α decays are responsible for the production of recoil nuclei (with
43 an energy ranging from 80 to 120 keV) and α particles (with an energy ranging from 4 to 6 MeV). The
44 glass is therefore submitted to dose rate and cumulative dose caused by these radiation sources, which
45 can damage the glass by accumulation of radiation effects into the glass structure.

46 There are many studies [7-10] on the impact of irradiation on the structure and the macroscopic
47 properties of borosilicate glasses including ISG glass (reference glass chosen by the international
48 scientific community). These studies have shown that nuclear effects are more efficient than electronic
49 ones to damage the glass structure [8]. It was shown that the maximum changes in the glassy state
50 (also called saturation damage state) are induced by nuclear collisions at a dose level of around 30 to
51 40 MGy, corresponding to around 500 years of radiation ageing of nuclear glass. Electronic effects
52 induced a lower damage level than nuclear effects and require a higher dose level of around 3GGy
53 (corresponding to of around several decades of radiation ageing of nuclear glass) to reach the
54 saturation damage state [8]. Moreover coupled effects between nuclear and electronic collisions have

55 been observed [8]. Indeed, the α particles induce a partial annealing of the damage generated by the
56 heavy ions. In addition, Angeli et al [11] studied the effect of hyperquenching on ISG glass fibers and
57 reported a disordered structure similar to that of induced by irradiation.

58

59 After a few hundred or even a few thousand years, water will access the cells containing the waste
60 packages. Then, the glass will evolve into an open system (presence of water), which represents a risk
61 of dissemination of radionuclides by water. It is thus of primary importance to assess the glass chemical
62 durability. Once the glass package is in contact with the groundwater, exchanges of chemical species
63 take place at the solid/solution interface leading to changes in the properties of the glass [4, 12, 13].
64 Several successive mechanisms occur at the glass/solution interface with different kinetics. Glass
65 hydration by diffusion of water in its structure precedes the interdiffusion step, which consists of an
66 ion exchange between the protons from the solution and the alkaline elements contained in a layer of
67 a few angstroms at the glass surface. Then, hydrolysis of the vitreous network consists of a nucleophilic
68 attack of a hydroxide ion OH^- on a bridging bond leading to the dissolution of the glass [14]. The
69 maximum alteration rate (called r_0) in a given environment is observed during the hydrolysis stage.

70 The impact of the recoil nuclei of α decays on the glass initial alteration rate regime has already been
71 partially addressed in the literature. Most studies are dedicated to glasses of complex composition and
72 did not show any effect of radiation on the initial alteration rate [15, 16]. Recent studies, rather focused
73 on simplified glasses, seem to indicate an impact of this type of irradiation at short alteration times
74 [17-19]. However, these studies did not fill all the gaps. Indeed, Karakurt et al.[17] studied the
75 alteration of ISG glass irradiated with 7 MeV Au ion up a fluency of $6.4 \cdot 10^{13} \text{at.cm}^{-2}$, but the first
76 measurements of altered depths were already beyond the irradiated zone (after 2 days reached $3 \mu\text{m}$,
77 so beyond the irradiated zone) and therefore the measured rates corresponded rather to non
78 irradiated glass. Zhang et al. [19] studied a simple 3-oxide glass, as well as Lonartz et al. [18]. In
79 addition, the ions used have a high energy whose representativeness of the effects of self-irradiation
80 by α decay is not yet fully demonstrated and the alteration conditions do not quite correspond to an

81 initial alteration regime. That's why this study focused on ISG glass (reference glass chosen by the
 82 scientific community), irradiated with 7 MeV gold ion irradiation in order to simulate the nuclear
 83 damage caused by recoil nuclei of α decays. In addition, the structural evolution of ISG submitted to
 84 this type of irradiation has already been described in the literature [8-10]. Leaching tests have been
 85 performed using low surface over solution volume ratio to determine the initial leaching rate of
 86 irradiated and non-irradiated ISG glass samples. The current article presents the experimental
 87 conditions, the results of the leaching tests and discusses the origin of the effect of the external
 88 irradiation on the leaching rate.

89

90 Materials and methods

91 Glass samples preparation

92 In this study, the alteration experiments were carried out on the International Simple Glass (ISG)
 93 provided by MoSCI Corporation (Rolla, Missouri, USA). Its composition is given in Table 1 [4].

94 *Table 1: ISG glass composition.*

Oxide	SiO ₂	B ₂ O ₃	Na ₂ O	Al ₂ O ₃	CaO	ZrO ₂	
wt %	56.2	17.3	12.2	6.1	5.0	3.3	
mol %	60.1	16.0	12.7	3.8	5.7	1.7	
Element	Si	B	Na	Al	Ca	Zr	O
wt %	26.3	5.4	9.0	3.2	3.6	2.4	50.1
mol %	18.0	9.6	7.6	2.3	1.7	0.5	60.3

95

96 Glass monoliths were obtained from a glass cylinder of 2 cm in diameter that was cut into six monoliths
 97 (more or less equivalent in size) which were polished to optical grade (1/4 micron finish) on both sides
 98 (up to reach a sample thickness of 700 μ m) and on the edge (Prime Verre company, Montpellier,
 99 France). Indeed, surface roughness may influence glass alteration [20, 21] therefore, it is necessary
 100 that the samples would be completely polished. The geometric surface area of the polished monoliths
 101 was considered in calculations of the normalized alteration rate.

102 Irradiation scenario

103 ISG glass monoliths were irradiated on both sides with 7 MeV Au³⁺ ions on the 2MV Aramis accelerator
104 at the SCALP facility (CNRS-CSNSM, Orsay, France) to induce a significant nuclear damage in the glass
105 structure as demonstrated in numerous studies that have been recently reviewed in [8]. A fluence of
106 2×10^{14} at.cm⁻² was used, which induces a minimum nuclear dose of around 40 MGy in the whole
107 irradiated depth [9] and thus to reach the saturation damage, i.e. the maximum damage level that can
108 be induced in a glass with nuclear collisions [8]. However, the concentration of Au ion in the glass is
109 very low in the present study (< 0.006 at.%) so that any chemical modification induced by Au on the
110 structure of the glass can be ruled out. The Au implantation profile was measured by negative ions
111 analysis by Time-of-Flight Secondary Ion Mass Spectrometry (ToF-SIMS) and was also obtained by
112 simulation with the Stopping and Range of Ions in Matter (SRIM) software [22]. It was shown that the
113 7 MeV Au³⁺ ions stop after a range of around 2 μm within the glass [9], creating thus a damage depth
114 of 2 μm thick. It is worth noting that the alteration protocol was chosen to generate an altered depth
115 less than or equal to the damaged depth so that the non-irradiated glass does not contribute to the
116 initial alteration rate value. However, in addition to the two main irradiated faces, the edges of the
117 sample which had not been irradiated and represented 10 % of the geometrical surface area
118 contributed to the release of elements in solution. Thus, a correction was achieved when calculating
119 the alteration rate (see equation 3).

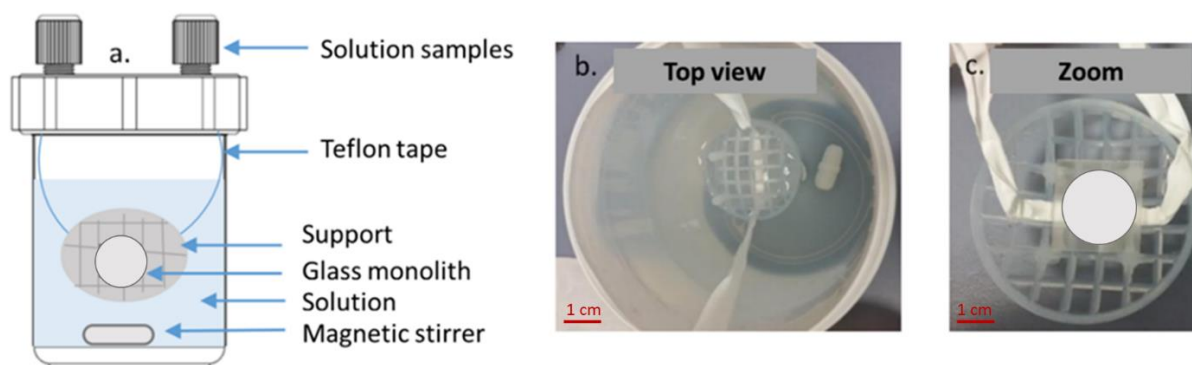
120

121 Alteration protocol

122 The leaching experiments were carried out in PFA (Perfluoroalkoxy) reactors, Savillex® brand. These
123 experiments were conducted on the non-irradiated ISG glass (named NI_glass later) and on the ISG
124 glass irradiated with Au-ion (named Au_glass later). The alteration experiments were performed in an
125 oven at 90°C and at a pH_{90°C} of 9.0 ± 0.2 . Several reasons explain the choice of this pH. Hydrolysis is a
126 mechanism closely linked to protonation and hydroxylation of the glass surface, in particular the

127 adsorption of OH^- on Si sites in basic media. This mechanism is clearly favored in basic media. In order
128 to be at a basic pH in a buffered solution (in order to remain the pH stable during the whole experiment
129 duration), to be close to the pH measured on long term leaching experiments implemented in initial
130 pure water and to have the possibility to compare our study to results in the literature, $\text{pH}_{90^\circ\text{C}} 9$ was a
131 good compromise.

132 The solution was continuously stirred thanks to a magnetic stirrer. The volume of solution
133 (approximately 670 mL) was adapted to the surface area of the coupon to reach the chosen surface
134 over solution volume ratio (SA/V) of 0.01 cm^{-1} . The pH 9 solution was prepared by adding 9.53 mg of
135 lithium hydroxide (99.995% purity, Alfa Aesar) into 1 L of deionized water. The pH was measured once
136 the solution was prepared, at 90°C , under strong stirring and reached 9.0 ± 0.2 . Then, the lithium
137 hydroxide solution was introduced into the Savillex® reactor that was placed for the night in an oven
138 at 90°C the day before the start of the experiment. At the beginning of the experiment, a PFA
139 holder was held in the middle of the leachate, using a Teflon ribbon. The glass monolith was finally
140 placed on this sample holder so it would be completely immersed in the solution. The complete set-
141 up is shown in Figure 1.



142

143 *Figure 1 : Schematic representation of a Savillex® reactor (a), top view of the reactor (b) and zoom on*
144 *the glass monolith on its holder (c).*

145

146 The alteration experiment lasted 24 hours but the initial alteration rate was calculated over the first 8
147 hours to guarantee a concentration in silicon less than 1 mg.L^{-1} . This choice was made to avoid the

148 influence of saturation phenomenon of the solution with respect to silica on the alteration rate [20].
149 In addition, for Au_samples, beyond 8 hours of alteration, the altered thickness became greater than
150 the irradiated depth (2 μm). This statement is done by calculating the altered depth from elemental
151 releases in solution, by applying equation (4). Moreover, to limit disruptions of the system, the number
152 of samples taken (one per hour) and each leachate sample volume (10 mL) were adapted to limit the
153 total sampled volume (less than 20 % of the total volume). Experiments on NI_glass and Au_glass were
154 repeated 3 times each.

155 Solution analyses

156 Under these conditions, all the elements coming from the glass are expected to be released in solution
157 (except zirconium which is very poorly soluble at a pH of 9.0) [23] and can be used to determine the
158 alteration rate. Measurements of the elemental concentrations were conducted using both UV-visible
159 spectrophotometry (Cary Varian 50 Scan) for Si and ICP-AES (Spectro Arcos EOP) for other elements.
160 For UV-visible spectroscopy measurements, commercial Spectroquant® kits were used to prepare the
161 standard solutions and unknown samples. The absorbance was measured at a wavelength of 665 nm
162 for silicon and 405 nm for boron using a UV-visible spectrophotometer. The absorbance measurement
163 was repeated 5 times to check the stability of the signal and an average of the 5 measurements was
164 retained. Calibration was done using several standard solutions prepared by dilution in deionized
165 water of commercial standard solutions at 1 g.L^{-1} (ARISTAR® single element calibration standard for
166 ICP-AES 1000 mg L^{-1} , VWR). The concentrations of the standard solutions were in the range from 0.1
167 to 2 mg.L^{-1} for B and from 0.5 to 5 mg.L^{-1} for Si. 9 mL of each sample was used for UV-visible
168 measurements and the remaining leachate sample (1 mL) was then acidified by adding a small amount
169 (about 70 μL) of 14 N nitric acid (Suprapur®, 14 N, 65%) to reach $[\text{HNO}_3] = 1 \text{ mol.L}^{-1}$ and analyzed by
170 ICP-AES. All analyses were carried out the day after the end of the experiment. Two to four
171 wavelengths per element were selected to measure the elemental concentration with ICP-AES. For
172 each wavelength, calibration curves were determined from the analysis of several standard solutions

173 prepared by dilution in 1 mol.L⁻¹ HNO₃ solution of certified standard solutions at 1 g.L⁻¹ (PlasmaCAL
174 single element calibration standard for ICP-AES 1000 mg L⁻¹, SCP-Science). Three measurements were
175 done for each selected wavelength. Then, the elemental concentrations were calculated as the
176 average of the results obtained for all wavelengths.

177 The relative experimental uncertainty on the concentration obtained by using UV-visible
178 spectrophotometry was estimated to 10 %. For ICP-AES analyses, it corresponded to twice the relative
179 standard deviation of the concentrations obtained for the different selected wavelengths (i.e. 5 % for
180 B, Na and 10 % for Ca and Al).

181 The normalized mass losses ($NL_i(t)$) for element i at time t were calculated from the concentrations
182 measured by UV-visible spectrophotometry or by ICP-AES, according to equation 1.

$$183 \quad NL_i(t) = \frac{c_i(t) \times V(t) + \sum_{j=1}^{t-1} [c_i(t) \times V_j]}{x_i \times S} \quad \text{with } V(t) = V_0 - \sum_{j=1}^{t-1} V_j \quad (1)$$

184 where: $C_i(t)$ is the concentration of element i measured in solution at time t (in g.L⁻¹); $V(t)$ is the volume
185 of solution remaining in the Savillex[®] reactor at time t (in L); V_j is the solution volume removed from
186 the reactor at each sampling time (in L); V_0 is the initial volume of solution in the reactor (in L); x_i is the
187 mass fraction of element i in the glass and S is the geometric surface area of the glass (in m²).

188 The alteration rate (r_i) for a given element i corresponds to the time derivative of the normalized mass
189 loss (equation 2). It is usually expressed in g.m⁻².d⁻¹.

$$190 \quad r_i = \frac{d(NL_i(t))}{dt} \quad (2)$$

191 The releases of the different elements of the glass were found to be congruent. Therefore, the effective
192 rate, $r_{\text{effective}}$ was calculated by averaging the results obtained for the various replicated leaching
193 experiments and all the elements (Si, B, Na, Ca, Al).

194 Moreover, a correction was performed to calculate the initial alteration rate in order to take into
195 account that 10 % of the geometric surface area (i.e. the edges) of the monolith was not irradiated.

196 The corresponding initial alteration rate of a monolith entirely irradiated with Au-ion, $r(\text{Au_glass})$, was
197 calculated using equation (3):

$$198 \quad r(\text{Au_glass}) = \frac{r_{\text{effective}} - 0.1 \times r(\text{NI-glass})}{0.9} \quad (3)$$

199

200 where $r(\text{NI_glass})$ is the alteration rate of the non-irradiated glass and $r_{\text{effective}}$ is the alteration rate
201 calculated from the experimental normalized mass losses of the monolith irradiated on the two main
202 faces.

203 The rate expressed in $\mu\text{m}\cdot\text{d}^{-1}$ is calculated from the rate expressed in $\text{g}\cdot\text{m}^{-2}\cdot\text{d}^{-1}$ by multiplying this latter
204 by the value of the ISG glass density, ρ , (expressed in $\text{g}\cdot\text{cm}^{-3}$):

$$205 \quad r(\text{in } \mu\text{m}\cdot\text{d}^{-1}) = r(\text{in } \text{g}\cdot\text{m}^{-2}\cdot\text{d}^{-1}) \times \rho(\text{in } \text{g}\cdot\text{cm}^{-3}) \quad (4)$$

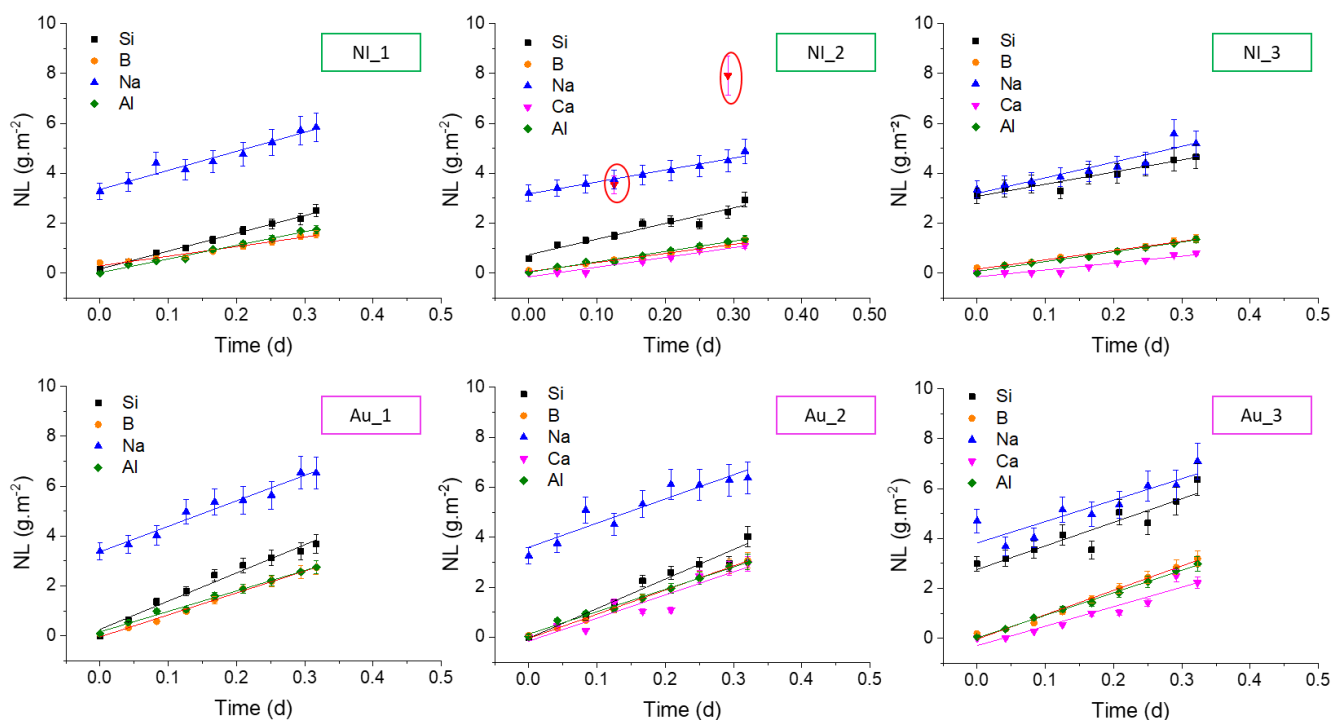
206 Results

207 The study of the initial alteration rate regime allows to focus on the first moments of the glass
208 alteration. This regime is controlled by hydrolysis of the vitreous network [14] and corresponds to a
209 maximum rate of alteration of a glass in a given medium.

210 From the releases in solution, the normalized mass losses were calculated for all the elements of the
211 glass and plotted as a function of the alteration time for the 6 samples in Figure 2. It is worth noting
212 that over a period of 8 hours, the evolution of normalized mass losses was linear, regardless of the
213 element considered and the type of sample considered (NI_glass or Au_glass). Congruency was
214 systematically observed for B, Al and Ca, while normalized mass losses in Na were systematically
215 higher. For Ca, outliers were attributed to potential contaminations (points drawn in red and framed)
216 and these data were not considered in the determination of the r_{Ca} . For NI_1 (NI_1 means Non-
217 Irradiated glass, test number 1) and Au_1 tests (Au_1 means Au irradiated glass, test number 1), the
218 releases of Ca were too scattered, therefore they were not considered in the subsequent calculations

219 of r_{Ca} . For Si and Na, the initial concentrations are variable. It was thus assumed that an initial
 220 contamination in the Savillex® reactor could have induced an initial offset of the concentrations. This
 221 initial offset had virtually no impact on the slope of the $NL_{Si}(t)$ and $NL_{Na}(t)$ curves. Thus, these data were
 222 used to determine r_{Si} and r_{Na} .

223



224 *Figure 2 : Normalized mass losses (NL) of the different glass elements as a function of the leaching time*
 225 *for the 3 experiments with NI_samples (NI_1,2,3) and with Au_samples (Au_1,2,3). The data circled in*
 226 *red were not used in the calculation of r_{Ca} .*

227

228 Linear regression was performed on the NL obtained for each element and the slopes corresponding
 229 to the initial rates are reported in

230 Table 2. We observed that, regardless of the element considered and the series, the results of the
 231 various experiments were not significantly different. The initial alteration rates calculated were
 232 systematically lower for NI_glasses than for irradiated Au_glasses. For NI_glasses, an average initial
 233 rate of $(4.9 \pm 3.0) \text{ g.m}^{-2}.\text{d}^{-1}$ was obtained compared to $(10.0 \pm 2.5) \text{ g.m}^{-2}.\text{d}^{-1}$ for the glasses irradiated
 234 with Au-ion. Therefore, there is a significant impact of Au-ion irradiation on the value of the initial

235 alteration rate. This impact led to an increase in the average initial alteration rate by a factor $F = 2.0 \pm$
 236 0.8 . This higher initial alteration rate in the case of ISG glass samples irradiated with Au-ion indicated
 237 a difference in chemical reactivity at the very first moments of alteration.

238

239 *Table 2: Initial alteration rate (r_i) in $\text{g}\cdot\text{m}^{-2}\cdot\text{d}^{-1}$ for each element of the glass and for each test. The ratio*
 240 *of the average initial alteration rates of irradiated samples to non-irradiated samples ($F =$*
 241 *$r(\text{Au_glass})/r(\text{NI_glass})$) is given in the last column of the table. The final rate (given in $\text{g}\cdot\text{m}^{-2}\cdot\text{d}^{-1}$ and*
 242 *$\mu\text{m}\cdot\text{d}^{-1}$) is the average of all the elements and all the tests. The $r_{\text{effective}}$ value is the calculated leaching*
 243 *rate without considering the non-irradiated edges. All uncertainties correspond to twice the standard*
 244 *deviation except for $r(\text{Au})$ where $\Delta r(\text{Au}) = \Delta r_{\text{effective}} + 0.1 \times \Delta r_{\text{NI}}$.*

245

$r_i(\text{g}\cdot\text{m}^{-2}\cdot\text{d}^{-1})$	NI_1	NI_2	NI_3	Au_1	Au_2	Au_3	F
Si	7.1	6.3	4.9	11.3	11.8	9.5	1.8
B	3.8	3.6	3.7	8.8	9.7	9.8	2.5
Na	7.6	4.8	6.3	10.2	9.7	8.6	1.5
Ca		3.9	2.8		9.2	7.8	2.2
Al	5.5	4.1	3.9	8.2	8.9	9.0	1.9
$r_{\text{effective}}(\text{g}\cdot\text{m}^{-2}\cdot\text{d}^{-1})$				9.5 \pm 2.2			
$r(\text{g}\cdot\text{m}^{-2}\cdot\text{d}^{-1})$	4.9 \pm 3.0			10.0 \pm 2.5			
$r(\mu\text{m}\cdot\text{d}^{-1})$	2.0 \pm 1.2			4.0 \pm 1.0			

246

247 Discussion

248

249 Initial alteration rate values of ISG glass

250

251 This study allows to determine the initial alteration rate of ISG at 90°C and at pH=9. It is important to
 252 note that only few data regarding the value of the initial alteration rate of ISG glass exist in the
 253 literature and that the published data are variable (see Table 3). Most of these data concern non-
 254 irradiated ISG specimens. Some studies were conducted on ISG glass powder (the surface area was
 255 measured by the BET method or using the geometric surface of the powder) and others on monoliths.
 256 In order to be able to compare the initial alteration rate values obtained for powders and for monoliths,
 257 it is necessary to use corrective factors as assessed by Fournier et al. [20]. Indeed, the initial alteration

258 rate obtained from the powder should be multiplied by a factor of 0.8 when the surface area
259 considered is the geometric one and by 1.9 when the surface area is measured by the BET method.

260 Jegou [24] studied the initial alteration rate of non-irradiated ISG glass powder altered in pure water
261 at 90°C, with SA/V = 0.1 cm⁻¹ and pH = 9, over 2 days. Jegou reported an initial alteration rate of $r_0=1.7$
262 g.m⁻².d⁻¹, which becomes $r_0(\text{monolith}) = 3.2 \text{ g.m}^{-2}.\text{d}^{-1}$, using the corrective factor recommended by
263 Fournier et al. [20].

264 Gin et al. [25] also altered ISG glass powder in initial rate regime in pure water at pH 9, 90°C, with a
265 SA/V ratio of 0.076 cm⁻¹ and for 5.7 h. They obtained a r_0 value of $8.2 \pm 2.5 \text{ g.m}^{-2}.\text{d}^{-1}$. After applying the
266 appropriate corrective factor of 0.8, the corresponding average rate for a monolith is $6.6 \text{ g.m}^{-2}.\text{d}^{-1}$.

267 Inagaki et al. [26] carried out leaching experiments at different pH and temperatures on ISG glass
268 monoliths and determined a relation between the alteration rate at 90°C and the pH ($\log r_{\text{Si}} = -1.56 +$
269 $0.236 \times \text{pH}$). The use of this relation for pH = 9 gave $r_{\text{Si}} = 3.7 \text{ g.m}^{-2}.\text{d}^{-1}$.

270 Fournier et al. [17] carried out leaching experiments at pH=10 and 90°C on ISG glass monoliths. Using
271 the relation between the alteration rate at 90°C and the pH ($\log r_{\text{Si}} = -1.56 + 0.236 \times \text{pH}$) [21], $r_{\text{Si}} = 3.9$
272 g.m⁻².d⁻¹.

273 Thus, considering data from the literature, the initial alteration rate of a non-irradiated ISG glass in
274 pure water at pH 9 and 90°C ranges from 3.2 to 6.6 g.m⁻².d⁻¹. The value obtained in this work for non-
275 irradiated ISG monoliths (i.e. $4.9 \pm 3.0 \text{ g.m}^{-2}.\text{d}^{-1}$) is well included in this range. This observation led to
276 the conclusion that the experimental protocol and the data treatment were reliable.

277

278

279

280

281

282 *Table 3 : r_0 values of ISG glass reported in the literature and from the current study. SPFT means Single-*
 283 *pass flow-through. Results from Neeway et al. were acquired at pH22°C 10 and 11, a mean value*
 284 *corresponding to pH90°C 9 (i.e. pH22°C 10.7) was extrapolated to be compared to our study.*

References	pH _{90°C}	Temperature (°C)	S/V (cm ⁻¹)	Powder or monolith?	Corrective factor	Leaching protocol	Time (d)	Corrected r_0 (g.m ⁻² .d ⁻¹)
Jegou 1998	9	90	0.1	Powder	×1.9	Static	2	3.2
Gin 2020	9	90	0.076	Powder	×0.8	Static	0.24	6.6 ± 2.5
Inagaki 2013	9	90		Monolith		Flow cell		3.7
Neeway 2018	~ 9	90		Powder		SPFT	21	2.9
This study	9	90	0.01	Monolith		Static	0.33	4.9 ± 3.0

285

286

287 To the best of our knowledge, there are only two studies reporting results on the initial alteration rate
 288 of ISG glass whose structure was damaged before alteration. Angeli et al. [11] studied ISG glass fibers
 289 hyperquenched (simulating structural disorder close to the one induced by irradiation) and therefore
 290 structurally more disordered. They showed that the silicate network, was hydrolyzed 1.4 to 1.8 times
 291 faster than for annealed fibers. This result is close to the increase factor obtained in this study, which
 292 is 2.0 ± 0.8 . However, the second study of Karakurt et al. [17] on the initial rate of ISG glass irradiated
 293 with gold ions cannot be considered since the glass was altered deeper than the irradiated zone.

294 Thus, the results obtained in our study brings new information and showed an effect of the glass
 295 disorder on its initial alteration rate and is consistent with the literature: the r_0 of an irradiated or
 296 hyperquenched ISG glass is increased compared to the one of a non-irradiated ISG glass.

297

298 [Origin of the rate difference between NI_glass and Au_glass](#)

299 The initial alteration rate of Au_glass samples was found to be higher than that of NI_glass by a factor
 300 of 2.0 ± 0.8 . This observation means that the chemical reactivity of the Au_glass with respect to the

301 solution (pure water) is greater than that of the NI_glass during the hydrolysis step. Several authors
302 [10, 11, 27, 28] showed that there is a link between the structural disorder of glass, whether thermally
303 induced [11] or by irradiation [10, 27, 28], and its chemical durability in the long term alteration rate
304 regime. The current study demonstrated that this is also true for the initial alteration rate of ISG glass.
305 Several explanations could be proposed to explain the increase of r_0 due to the glass disorder induced
306 by Au-ion irradiation.

307 Firstly, radiation damage as well as high quenching rate induce a modification of the glass short range
308 order (SRO) with the creation of point defects (electronic defects on atoms or bonds in the glassy
309 network, often called color centers) and non-bridging oxygen atoms that induce a decrease of the
310 polymerization of the glass network. Moreover a partial conversion of BO_4 (B(+IV)) to BO_3 (B(+III))
311 species [7, 9-11, 18, 29, 30] is observed that also participates to the decrease of the glass
312 polymerization degree which could induce a higher hydrolysis of the silicate network and result in an
313 increase in glass alteration rate. Overall, the general depolymerisation of the glass network results in
314 a lower number of bridging bonds between network former atoms. The initial rate regime is controlled
315 by the hydrolysis of the vitreous network through the breaking of its bridging bonds (Si-O-Si, Si-O-Al
316 or Si-O-Zr for example) by protonation or hydroxylation of reactive surface sites [14]. Thus, the
317 hydrolysis of the glass can be favoured by a low degree of polymerization of the vitreous network. This
318 was recently confirmed by Monte Carlo simulations which showed that the primary cause for the
319 increase of glass alteration rate was the extent of the depolymerization of the glass network
320 introduced by these local structural changes (boron coordination, number and nature of Q^n species,
321 and angular distribution of Si-O-Si linkages) [31]. Moreover the reactivity of B(III) was shown to be
322 higher than that of B(IV). Kapoor et al. [32] showed that the boron (+III) could be seen as a Lewis acid,
323 with water acting as a Lewis base. Moreover, by considering the Lewis acido-basicity of borate species,
324 an increased reactivity of the B(+III) compared to B(+IV) can be assumed to increase the glass network
325 hydrolysis.

326 Secondly, the radiation damage generated by nuclear collisions also induces a modification of the glass
327 medium range order (MRO) with mainly a broadening of the ring size and angle distribution [10, 33],
328 as indicated by the increase of three membered silicate rings and the shift of R band (which
329 corresponds to bending and rotation modes of Si-O-Si bands). The MRO modification was also
330 observed by molecular dynamic simulation of radiation damage and high quenching rate in simple
331 borosilicate glasses [34]. This modification of the ring size distribution directly affects the glass free
332 volume and thereby the accessibility of the water into the glass network [34], that may also favour its
333 hydrolysis.

334 Finally, the modification of short and medium range orders can occur either upstream of the hydrolysis
335 step, the water penetrates faster into the glass and therefore leads to a deeper hydrolysis [35] or are
336 directly related to the increase of B(III), more reactive towards water [29, 32]. These two processes
337 can effectively act concomitantly and synergistically.

338

339 [Comparison between ISG and SON68 complex nuclear glass](#)

340 In the literature, it was shown for SON68 glass that irradiation with Au-ion had no significant impact
341 on the initial alteration rate [15]. Indeed, the initial rate of SON68 glass was about $2 \text{ g}\cdot\text{m}^{-2}\cdot\text{d}^{-1}$, whether
342 the glass was irradiated with Au-ion or not [15], which was also the case for SON68 glasses doped with
343 actinides [15, 16, 36]. The more complex chemical composition of SON68 glass compared to ISG glass
344 may have a role in the weaker impact of Au-ion on the glass structure and thus on the initial alteration
345 rate [8], because it could favour a higher degree of chemical mixing and random organisation of the
346 glassy network that could reduce the glass sensitivity to nuclear damage, that induce a ballistic mixing
347 of the material due to the displacements cascades. More experiments on complex SON68 glass are
348 needed to quantify its structural evolution versus irradiation and compare it to the one of ISG glass so
349 as to try to explain the lower sensitivity of SON68 glass initial alteration rate under irradiation.

350

351 Conclusion

352 This study was dedicated to the impact of nuclear collisions (simulating the effects of the recoil nuclei
353 of α decays) on the initial alteration rate of the ISG glass. It was shown that the initial alteration rate
354 of the ISG glass irradiated with 7 MeV Au-ion was 2.0 ± 0.8 times higher than that of a non-irradiated
355 ISG glass. This work demonstrated that there is a link between the structural changes of ISG glass
356 caused by nuclear collisions and its initial alteration rate. The origin of the increase of the alteration
357 rate seems to be associated to the short and medium range order changes induced by the nuclear
358 collisions, and certainly by the amplitude of the boron coordination change (B(IV) to B(III)). Similar
359 irradiation conditions on SON68 glass did not induce any changes of its alteration rate which suggests
360 that the more the structure of the glass is modified by irradiation (change in boron coordination,
361 change in NBO), the higher the alteration rate of the glass is.

362 Subsequently, it would be interesting to continue the investigation of the structural changes induced
363 by irradiation on more complex glasses, up to SON68 one, in order to identify the glass composition
364 domain that did not show any dependence of its initial alteration rate with irradiation.

365 Acknowledgments

366 The authors would like to thank Pascale Colombel and Laurent Duffours (Prime Verre company,
367 Montpellier, France) for sample preparation, Jérôme Bourçois (CNRS-CSNSM, Orsay, France) and
368 Olivier Cavani (Ecole Polytechnique, Palaiseau, France) for carrying out irradiations, Elodie Chauvet and
369 Loan Lai (Tescan Analytics, Fuveau, France) and Laurent Dupuy (SERMA Technologies, Ecully, France)
370 for the ToF-SIMS characterizations. This work was performed in the framework of the Vestale project
371 co-funded by EDF, CEA and Orano and it was supported by INWARD coordinated research project [Ion
372 Beam Irradiation for High Level Nuclear Waste Form Development, F11022] from IAEA.

373

374

375

376

377 References

- 378 1. Gin, S., et al., *Radionuclides containment in nuclear glasses: an overview*. Radiochimica Acta, 2017. **105**(11): p. 927-959.
- 379
- 380 2. IAEA, France - *Sixth National Report on Compliance with the Joint Convention Obligations*. 2017, Joint Convention on the safety of the management of spent fuel and on the safety of the management of radioactive waste.
- 381
- 382
- 383 3. IAEA, *Status and Trends in Spent Fuel and Radioactive Waste Management*, ed. N.E.S.N. NW-T-1.14. 2018, Vienna.
- 384
- 385 4. Gin, S., et al., *An international initiative on long-term behavior of high-level nuclear waste glass*. Materials Today, 2013. **16**(6): p. 243-248.
- 386
- 387 5. ANDRA, *site internet de l'Agence Nationale pour la gestion des Déchets Radioactifs* :
- 388 www.andra.fr.
- 389 6. Weber, W.J., et al., *Radiation effects in glasses used for immobilization of high-level waste and plutonium disposition*. Journal of Materials Research, 1997. **12**(8): p. 1946-1978.
- 390
- 391 7. Peugeot, S., J.M. Delaye, and C. Jegou, *Specific outcomes of the research on the radiation stability of the French nuclear glass towards alpha decay accumulation*. Journal of Nuclear Materials, 2014. **444**(1-3): p. 76-91.
- 392
- 393
- 394 8. Mir, A.H. and S. Peugeot, *Using external ion irradiations for simulating self-irradiation damage in nuclear waste glasses: State of the art, recommendations and, prospects*. Journal of Nuclear Materials, 2020. **539**: p. 152246.
- 395
- 396
- 397 9. Gillet, C., et al., *Impact of complex irradiation scenarios on the structure and the properties of the International Simple Glass*. Journal of Nuclear Materials, 2022. **572**: p. 154079.
- 398
- 399 10. Peugeot, S., et al., *Radiation effects in ISG glass: from structural changes to long term aqueous behavior*. npj Materials Degradation, 2018. **2**:23.
- 400
- 401 11. Angeli, F., et al., *Effect of thermally induced structural disorder on the chemical durability of International Simple Glass*. npj Materials Degradation, 2018. **2**(1): p. 31.
- 402
- 403 12. Frugier, P., et al., *SON68 nuclear glass dissolution kinetics: Current state of knowledge and basis of the new GRAAL model*. Journal of Nuclear Materials, 2008. **380**(1-3): p. 8-21.
- 404
- 405 13. Gin, S., et al., *Insights into the mechanisms controlling the residual corrosion rate of borosilicate glasses*. npj Materials Degradation, 2020. **4**(1): p. 41.
- 406
- 407 14. Gin, S., et al., *The controversial role of inter-diffusion in glass alteration*. Chemical Geology, 2016. **440**: p. 115-123.
- 408
- 409 15. Peugeot, S., et al., *Effect of alpha radiation on the leaching behaviour of nuclear glass*. Journal of Nuclear Materials, 2007. **362**(2-3): p. 474-479.
- 410
- 411 16. Tribet, M., et al., *Irradiation Impact on the Leaching Behavior of HLW Glasses*. Procedia Materials Science, 2014. **7**: p. 209-215.
- 412
- 413 17. Karakurt, G., *Effect of alpha radiation on the physical and chemical properties of silicate glasses*. 2014, Thèse de l'Ecole des Mines de Nantes.
- 414
- 415 18. Lonartz, M.I., et al., *The Effect of Heavy Ion Irradiation on the Forward Dissolution Rate of Borosilicate Glasses Studied in Situ and Real Time by Fluid-Cell Raman Spectroscopy*. Materials, 2019. **12**(9): p. 1480.
- 416
- 417
- 418 19. Zhang, X.Y., et al., *Influence of ion radiation on leaching behavior of borosilicate glass*. Journal of Non-Crystalline Solids, 2023. **602**: p. 122091.
- 419
- 420 20. Fournier, M., et al., *Glass dissolution rate measurement and calculation revisited*. Journal of Nuclear Materials, 2016. **476**: p. 140-154.
- 421
- 422 21. Thien, B.M.J., G. Kosakowski, and D.A. Kulik, *Differential alteration of basaltic lava flows and hyaloclastites in Icelandic hydrothermal systems*. Geothermal Energy, 2015. **3**(1): p. 11.
- 423
- 424 22. Ziegler, J.F., J.P. Biersack, and M.D. Ziegler, *SRIM, the stopping and range of ions in matter*. 2008, Chester, Maryland: SRIM Co.
- 425

- 426 23. Brown, P.L., E. Curti, and B. Grambow, *Chemical Thermodynamics of Zirconium*, ed. C.T. 8.
427 2005.
- 428 24. Jegou, C., *Mise en évidence expérimentale des mécanismes limitant l'altération du verre R7T7*
429 *en milieu aqueux. Critique et proposition d'évolution du formalisme cinétique*. 1998, Thèse de
430 l'Université Montpellier II. p. [330 p.] Pagination multiple.
- 431 25. Gin, S., et al., *Can a simple topological-constraints-based model predict the initial dissolution*
432 *rate of borosilicate and aluminosilicate glasses?* npj Materials Degradation, 2020. **4**(1): p. 6.
- 433 26. Inagaki, Y., et al., *Initial Dissolution Rate of the International Simple Glass as a Function of pH*
434 *and Temperature Measured Using Microchannel Flow-Through Test Method*. International
435 Journal of Applied Glass Science, 2013. **4**(4): p. 317-327.
- 436 27. Mougnaud, S., et al., *Heavy ion radiation ageing impact on long-term glass alteration*
437 *behavior*. Journal of Nuclear Materials, 2018. **510**: p. 168-177.
- 438 28. Tribet, M., et al., *Alpha dose rate and decay dose impacts on the long-term alteration of HLW*
439 *nuclear glasses*. npj Mater. Degrad., 2021.
- 440 29. Stone-Weiss, N., et al., *Understanding the structural drivers governing glass-water*
441 *interactions in borosilicate based model bioactive glasses*. Acta Biomaterialia, 2018. **65**: p.
442 436-449.
- 443 30. Chen, L.T., et al., *Radiation effects on structure and mechanical properties of borosilicate*
444 *glasses*. Journal of Nuclear Materials, 2021. **552**: p. 153025.
- 445 31. Jan, A., et al., *Monte Carlo simulation of the corrosion of irradiated simplified nuclear waste*
446 *glasses*. Journal of Non-Crystalline Solids, 2019. **519**: p. 119449.
- 447 32. Kapoor, S., et al., *Structural and Chemical Approach toward Understanding the Aqueous*
448 *Corrosion of Sodium Aluminoborate Glasses*. Journal of Physical Chemistry B, 2018. **122**(48):
449 p. 10913-10927.
- 450 33. Karakurt, G., et al., *Understanding of the mechanical and structural changes induced by alpha*
451 *particles and heavy ions in the French simulated nuclear waste glass*. Journal of Nuclear
452 Materials, 2016. **475**.
- 453 34. Delaye, J.M., et al., *Comparative effects of thermal quenching and ballistic collisions in SiO2-*
454 *B2O3-Na2O glass*. Nuclear Instruments & Methods in Physics Research Section B-Beam
455 Interactions with Materials and Atoms, 2014. **326**: p. 256-259.
- 456 35. Mansas, C., et al., *Drivers of Water Transport in Glass: Chemical or Topological Effect of the*
457 *Glass Network?* The Journal of Physical Chemistry C, 2017. **121**(30): p. 16201-16215.
- 458 36. Wellman, D.M., J.P. Icenhower, and W.J. Weber, *Elemental dissolution study of Pu-bearing*
459 *borosilicate glasses*. Journal of Nuclear Materials, 2005. **340**(2-3): p. 149-162.

460

461

462

463

464

465

466

467

468

469